Applied Nanoscience (2021) 11:1349–1358
https://doi.org/10.1007/s13204-021-01774-y

ORIGINAL ARTICLE

Facile synthesis of cellulose–ZnO-hybrid nanocomposite using *Hibiscus rosa-sinensis* leaf extract and their antibacterial activities

Elias E. Elemike[1] · **Damian C. Onwudiwe**[2] · **Justina I. Mbonu**[1]

Received: 19 December 2020 / Accepted: 3 March 2021 / Published online: 13 March 2021

Abstract

Cellulose, zinc oxide nanoparticles (ZnO NPs) and a new composite of crystalline cellulose–ZnO nanoparticles (ZnO/CNC) have been prepared by simple hydrothermal treatment using Hibiscus leaf extract. The cellulose which was isolated from corn cobs and the nanomaterials were characterised using different analytical techniques including Fourier-transform infrared spectroscopy (FTIR), scanning electron microscopy (SEM), energy-dispersive X-ray spectroscopy (EDX), X-ray diffraction (XRD) measurements and transmission electron microscopy (TEM). These techniques explained the structure, crystallinity and purity of the extracted cellulose, ZnO NPs and the ZnO/CNC nanocomposite. The TEM image showed the rod like shape of the synthesized ZnO NPs with approximate width size of about 90.83 nm and length 546.97 nm, whereas the ZnO/CNC nanocomposite is of 4.89 nm spheroidal shape. The antibacterial properties of the as-synthesized nanomaterials showed good properties but the cellulose did not.

Keywords Biomaterials · Zinc oxide · Nanocomposites · Characterization · Morphological stability

Introduction

Cellulose can be isolated from various agricultural products and wastes. The isolation of cellulose from corn cobs is a way of utilizing agricultural wastes and the cellulose serves as supporting materials in different industrial applications. Some of the applications include in paper, cosmetics, paperboards, films, coatings, pharmaceutics, foods and textiles (Mun et al. 2016). In medicine, cellulose and their derivatives can be used as drug carrier and in wound healing due to their biocompatibility (Crabbe-Mann et al. 2018).

Due to the numerous hydroxyl group content of cellulose and their dipolar nature, it has been reported that they can be modified to possess ion migration effect and piezoelectric properties which hitherto will diversify their applications (Kim et al. 2006). The ordered hydroxyl groups are also connected by hydrogen bonds which offers high crystallinity, improves mechanical strength and makes the cellulose insoluble in water (Lennholm and Henriksson (2007)). Cellulose and nanocellulose are available, sustainable, abundant with good mechanical properties, large surface-to-volume ratio, great flexibility, tensile strength and stiffness, and good thermo-electrical properties (Vartiainen et al. 2011; Börjesson and Westman 2015). The European Food Safety Authority and the U.S. Food and Drug Administration have considered cellulose and some of their modified forms safe to handle and consume and can serve as additives in food and health care products (Food Standards Agency, 2014).

Zinc oxide nanoparticles is one of the most extensively used semiconductor materials with wider applications in photocatalysis, biomedicine, optoelectronics, photovoltaics and energy (Awan et al. 2018; Naseer et al. 2020; Siddiqi et al. 2018; Sirelkhatim et al. 2015). There is ease of manipulation and confinement of the electrons (e^-) and holes (h^+) in ZnO NPs which activates their redox functionalities (Awan et al. 2018; Naseer et al. 2020; Siddiqi et al. 2018; Sirelkhatim et al. 2015). ZnO NPs are generally regarded as safe nanomaterial; they have antimicrobial properties and are often used more than other metals or metal oxide nanoparticles in biomedicine, animal feeds and other organism-related applications (Yusof et al. 2019). Moreover, they are also easily and efficiently prepared using the biosynthetic procedure. The size effect of ZnO nanoparticles can lead to

✉ Elias E. Elemike
chemphilips@yahoo.com; elemike.elias@fupre.edu.ng

[1] Department of Chemistry, College of Science, Federal University of Petroleum Resources, Effurun, Nigeria

[2] Department of Chemistry, North West University Mafikeng Campus, Mafikeng, South Africa

charge redistribution in the material surfaces and eventual local polarization (Agrawal and Espinosa 2011).

ZnO nanostructures can be utilized as building blocks in nanocomposites. The impregnation of zinc oxide nanoparticles into cellulose to form nanocomposites is a great improvement in nanotechnology due to the synergistic contribution of the properties of the individual materials in one material. In the case of cellulose–ZnO nanocomposites, the incorporation of the ZnO into the cellulose may lead to structural deformation and modifications offering entirely new properties from the contributing materials (Sharma et al. 2010).

There are few studies on cellulose–ZnO nanocomposites but in recent times, research on this area is tremendously growing with different preparation methods (Lefatshe et al. 2017; Martins et al. 2013; Ul-Islam et al. 2014). Matharu et al. in their review work have opined that zinc oxide can be incorporated into cellulose to give different forms ranging from filaments, papers and foams and that the antimicrobial efficacy of the nanocomposites depends on the concentration of ZnO NPs in the composites (Matharu et al. 2018).

Azizi et al. (2013) have prepared ZnO-Ag/cellulose nanocrystal nanocomposites with improved antimicrobial activity and thermal stability (Azizi et al. 2013). Fu et al. (2015) also prepared cellulose–ZnO nanocomposite films using one-step coagulation method (Fu et al. 2015). The nanocomposites were verified for antibacterial properties and was found out to entirely destroy *Staphylococcus aureus* and *Escherichia coli* in 6 h of exposure. The inculcation of ZnONPs into the cellulose polymer would lead to some physicochemical changes (adhesion, wettability) of the new nanohybrid different from the individual materials and responsiveness to external effects or conditions (Wang et al. 2020). In a typical nanocomposite, the numerous OH contained in the cellulose interacts with the Zn^{2+} leading to surface modification of the nanocomposite for possible improved activities.

In this work, we employed ubiquitous, low-cost, biomediated and environmentally friendly plant extract (*Hibiscus rosa-sinensis*) in the synthesis of ZnO–cellulose nanocomposite. The novelty of the work lies on the use of available and sustainable plant material, safe metal salt and cellulose from agric-waste to form a nanomatrix. The idea is to develop nanocomposites capable of having enhanced antibacterial performance using model organisms such as *Staphylococcus aureus* and *Escherichia coli.* Cellulose and ZnONPs used in this work are biosafe and biocompatible. ZnONPs have also been reported to have good antibacterial properties which depend on the method of preparation, particle sizes, morphologies and concentration. The electrostatic interaction which exists between cellulose and ZnO is a great factor that aids the dispersion of the ZnO NPs within the cellulose material in the composites (Abdalkarim et al. 2018a).

Hibiscus rosa-sinensis (HR) is an invaluable plant with great biological importance. Among other pharmacological efficiency, it also possesses antimicrobial activities. Phytochemical analysis of the plant has shown the presence of phenolics, alkaloids, saponins, flavonoids, tannins, steroids, anthraquinones, quinines and so on (Ruban and Gajalakshmi 2012; Al-Snafi 2018). These metabolites have good reducing properties, possess functional groups that can modify the surface of metals or other materials. They are, however, used as green reducing agents instead of toxic chemical agents during synthesis of nanoparticles.

It is, therefore, our interest to synthesize HR-mediated ZnO nanoparticles and corn cob-derived cellulose to form nanocomposites for improved antimicrobial efficacy. There are different methods in which nanoparticles and their composites can be prepared but in this work, the biological means of using plant extract was followed. Since the nanocomposites are for biological applications, it is important that materials, chemicals and solvents that will be toxic to the biological organisms are avoided during the synthesis. Chemical agents, however, are toxic and may be gradually released in the host organisms after administration.

Materials and methods

Materials

Corn cobs, *Hibiscus rosa-sinensis* leaf, ethanol, Zinc acetate NaOH, HCl, NaOCl. The chemicals which were of analytical grade were obtained from BDH England and used as obtained.

Extraction of cellulose and removal of lignocellulose material

The corn cobs were initially washed, dried and ground to powder. The powdered biomass (5 g) was de-waxed using 100 mL of absolute ethanol and further treated with solution of 4% NaOH for 2 h at 90 °C. The lignin and other impurities were dissolved during this treatment and decanted off, thereafter washed with distilled water, rinsed and dried. The procedure was repeated to obtain purer product. The hemicellulose and lignin content of the material were further removed using 30% HCl at 45 °C for an hour.

Both acid and alkaline treatment exposed the surface area of the material thereby enabling good interfacial adhesion and fiber wetting (Kalia et al. 2009). The isolated cellulose material was bleached using 3.5% sodium hypochlorite and was done severally until the fibers became white. Bleaching improves the physical appearance of fibers and also mechanical properties thereby leading to enhancement in

fiber matrix interfacial adhesion (Rayung et al. 2014). The cellulose was filtered, washed severally and air-dried.

Synthesis of zinc oxide nano-particles

Hibiscus rosa-sinensis leaves were obtained from Effurun Delta State Nigeria, washed completely with plenty of distilled water and air-dried for 1 week. The leaves were ground and about 5 g was used in preparing aqueous extract in 100 mL of distilled water for 30 min at 50 °C. The extract was filtered and the filtrate used as bioreductant for preparation of nanoparticles.

Zinc acetate obtained from BDH England was used for the synthesis of ZnO nanoparticles. During the synthesis of zinc oxide nanoparticles (ZnO NPs), 1.8348 g (0.01 M) zinc acetate was dissolved in 1000 mL of distilled water (Elemike et al. 2019; Adeyemi et al. 2019). The prepared aqueous extract (50 mL) was introduced into 500 mL of the 0.01 M zinc acetate solution with 5 mL of 1 M NaOH. The reaction was heated and stirred at 80 °C for 4 h. The colloidal solution changed from yellowish to cream-colored precipitate of zinc hydroxide. Then the precipitate was collected by centrifugation at 4000 rpm and dried in an oven for 24 h at 50 °C to get rid of water and obtain the ZnO NPs.

Preparation of ZnO/cellulose nanocomposite (ZnO/CNC)

In the preparation of the cellulose–ZnO nanocomposite, 0.4 g of the isolated cellulose was introduced into the 0.01 M zinc acetate aqueous solution and stir-heated at 60 °C for 3 h. The solution was centrifuged and washed severally with distilled water to obtain the nanocomposites which was dried in an oven for 4 h at 60 °C. The mechanism and pathway of the reaction is shown in Scheme 1.

Characterization of the nanoparticles and nanocomposites

Different characterization techniques were used to identify the synthesized compounds. The FTIR spectroscopic characterization was done with the aid of Bruker alpha-P FTIR spectrometer operated in the range of 4000–400 cm^{-1}. In this model of FTIR, no sample preparation was done, the solid samples were just spread on the attenuated total reflection (ATR) diamond crystal surface and stamped by pulling the handle which allows the machine to scan through the sample thereby producing the spectra. The crystallinity of the cellulose, the nanoparticles and nanocomposites was determined using powder X-ray diffraction (pXRD) techniques of the model, automated Röntgen PW3040/60 X'Pert Pro X-ray diffractometer operated at room temperature with nickel-filtered Cu ($\lambda = 1.542$ Å) within 2θ value of 10°–80° at a scanning rate of 2° min^{-1} under voltage and current conditions of 40 kV and 30 mA, respectively. The morphological patterns and possible elemental composition of the materials were determined using Quanta FEG 250 Environmental scanning electron microscope (SEM) coupled with energy-dispersive X-ray spectroscopy (EDXS) operating at acceleration voltage of 30 kV. The solid samples were dispersed on the sample stumps while depositing thin gold layer on them for better electrical conductivity in order to give clear

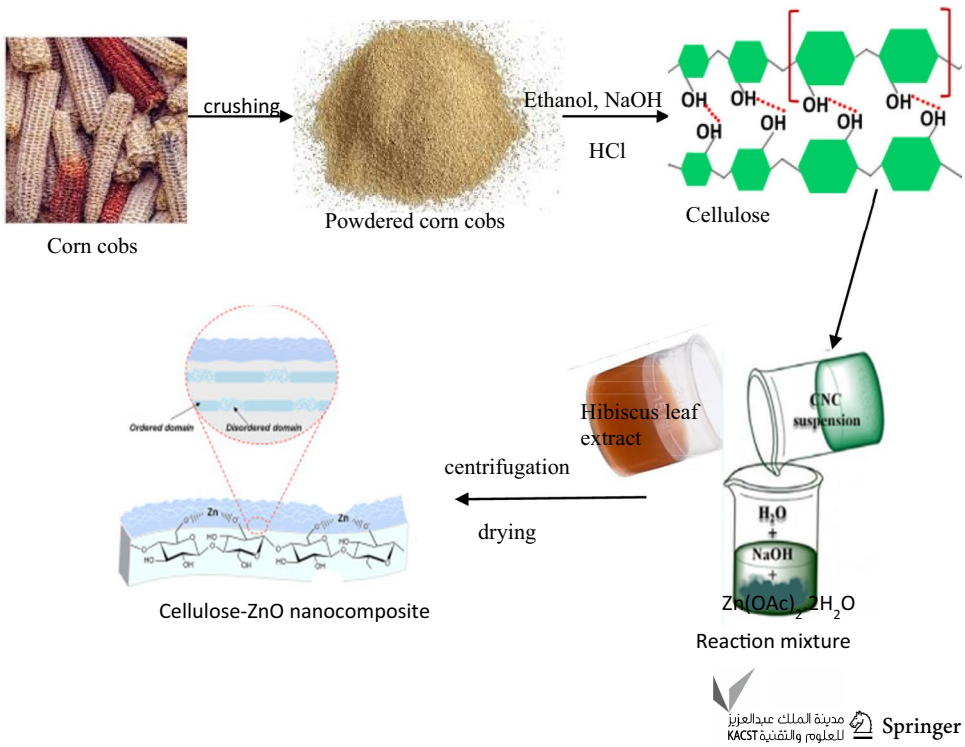

Scheme 1 Reaction pathway for the synthesis of cellulose–ZnO nanocomposite

images (Elemike et al. 2017). The model JEOL2100 transmission electron microscope (TEM) instrument which has LaB 6 electron gun fitted to it and operated at an acceleration voltage of 5 kV was used to determine the possible particle sizes of the nanocomposites. The samples were sonicated in water for an hour, sample was dropped on copper grids and dried while the image was captured with the Gatan Ultrascan digital camera attached to the TEM machine. The nanoparticle sizes were further determined with Image J software.

Antibacterial analysis of ZnO NPs and the composite materials

The antibacterial performance of the ZnO NPs and the cellulose–ZnO nanocomposite was assessed using the Agar-well diffusion method. Gram-negative *Escherichia coli* and Gram-positive *Staphylococcus aureus* were the model bacterial organisms used in this study. The culture medium for the test microorganisms was prepared with 17 g of agar, 15 g of beef extracts, 5 g of peptone, 5 g of NaCl and 1000 mL H_2O under the reaction pH value of 8.0. The cultured medium was poured into sterilized plates and allowed to solidify. About 0.2 mL of the model organisms (bacteria) (2×10^8 CFU/mL) each were streaked on the cultured plates and incubated for 24 h at a temperature of 37 °C (Zou et al. 2018; Du et al. 2018). A certain amount of about 0.1 mg/mL of the ZnO NPs, cellulose-ZnO nanocomposites and control drug (streptomycin) were introduced into the plates, sterilized in an autoclave and incubated for 24 h at 37 °C. The zone of inhibition of growth of bacterial organisms offered by the nanomaterials was measured in mm.

Results and discussion

FTIR spectra results

FTIR spectroscopic studies was used to monitor the changes from the corn cobs to the cellulose and the effect of the plant extract on the synthesis of the ZnO NPs and all through to the formation of the nanocomposites as represented in Fig. 1. The figure shows the FTIR of the crushed corn cobs, isolated cellulose from the corn cobs, ZnO NPs synthesized using *Hibiscus rosa-sinensis* and the nanocomposite made from the ZnONPs and the cellulose. In the FTIR of the crushed corn cobs there are prominent bands at 3685, 1739, 1600, 1499, 1040 cm^{-1}. The bands at 3685 cm^{-1} obviously reflect functional groups of OH typical of cellulosic content of the corn cobs, whereas the 1739 cm^{-1} may be due to carbonyl or ether functional group. The characteristic bands around 1600–1499 cm^{-1} could be attributed to aromatic ring stretch and/or probably methyl/methylene bend possibly arising from lignin and hemicellulose in the corn cobs. In

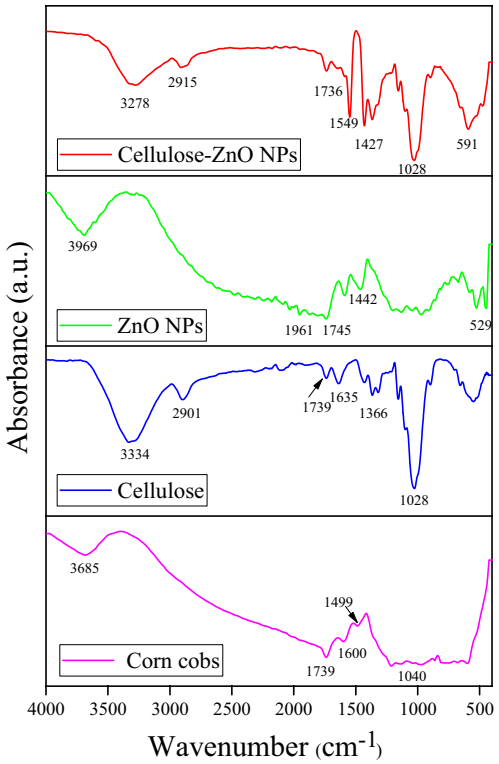

Fig. 1 FTIR spectra of the pulverized corn cobs, cellulose extracted from the corn cobs, ZnO NPs prepared using *Hibiscus rosa-sinensis* and cellulose–ZnO nanocomposites

the FTIR of the extracted cellulose, similar bands as the corn cobs occurred but with some interesting difference as the 3334 cm^{-1} band attributed to OH was more prominent and intense which showed bonded OH in cellulose (Morawski et al. 2013). The 2901 cm^{-1} band is due to C–H stretching vibrations, whereas the 1739 and 1635 cm^{-1} are characteristic carbonyl bands attributed to lactone ring and also typical of C–O bending (Wang and Shaw 2014). The OH in plane bend may be due to the band at 1366 cm^{-1}, while the prominent band at 1028 cm^{-1} is a characteristic of C–O stretch. The band around 552 cm^{-1} may be due to C–H stretch.

The spectrum obtained for the cellulose is well comparable to commercial cellulose with peaks 3391, 2906, 1760, 1654, 1373 and 1162 cm^{-1} (Abderrahim et al. 2015). From the spectrum of the ZnO NPs mediated by the *Hibiscus* leaf extract, it is obvious that the plant extract did not only reduce the zinc salt but also capped the nanoparticles as some bands could be attributed to the functional groups of the components of the leaf. The observed band at 3696 cm^{-1} may be assigned to O–H stretch due to water adsorption on the Zn metal surface. The bands at 1961 and 1442 cm^{-1} could be due to methyl/methylene stretch and bending vibrations, respectively, whereas the 1745 cm^{-1} band may be due to carbonyl group (Sirviö et al. 2017). These bands possibly may have emanated from the plant extract. The prominent

529 cm^{-1} band simply arises from Zn–O metal deformation. In the spectrum of cellulose–ZnO nanocomposite, various bands appeared at 3278, 2915, 1736,1549,1427,1028 and 591 cm^{-1}. These bands reflect both the components of cellulose, *Hibiscu*s leaf extract and ZnO. The 3278 cm^{-1} characteristic OH band appeared at a lower wavelength compared to the cellulose, an indication of formation of bond between the surface of the metal and the OH of the cellulose. Other characteristic bands such as the 1736 and 1028 cm^{-1} appeared and they are due to carbonyl or C–O stretch. The Zn–O metal bond is observed at 591 cm^{-1} which occurred at a higher wavenumber compared to the 529 cm^{-1} band in the ZnO NPs due to composite formation. The red shift could also be due to variation in size and crystalline structure of cellulose–ZnO nanocomposites (Abdalkarim et al. 2018b).

X-ray diffraction (XRD) result

Figure 2 shows the pXRD patterns of the powdered corn cobs, isolated cellulose, ZnO NPs and the cellulose–ZnO nanocomposites. The nature of the peaks showed some changes in the figure. In the spectrum of the native corn cobs, some crystallinity associated with the material was observed as reflected in the peaks at $2\theta = 22.65$ and 34.88° attributed to (200) and (040) crystal planes, respectively. In the spectrum of the isolated cellulose, the $2\theta = 15.89$, 22.65 and 34.88° corresponding to (110), (200) and (040) planes, respectively, were sharper and purer with the major peak at 22.65 which is in tandem with the report of Trilokesh and Uppuluri (2019; Li et al. 2012). The improved crystallinity of the cellulose leads to surface roughness which enhances material adhesion. This observed peak at $2\theta = 27$ may be due to cellulose I allomorph or unidentified impurity phases or aromatic layer structure of carbon (graphite 002) (Jawada et al. 2018; Zheng et al. 2014).

The dried sample of the ZnO NPs was used to determine the crystallinity of the synthesized nanoparticles. The observed spectrum showed well-defined peak linked to the material of investigation with single-phase nature devoid of secondary phases. Major significant peaks at 2θ values = 32.01, 34.60, 37.28, 47.62, 56.67, 63.47, 66.47, 68.11, and 69.17° corresponding to (100), (002), (101), (102), (110), (103), (200), (201) and (112) planes, respectively, were seen. The nature of the peaks reflects the wurtzite hexagonal crystallographic ZnO lattice structure (JCPDS file no 36-1451) which is similar to the reports of Chaudhuri et al. (2017).

In the X-ray diffraction (XRD) pattern of the synthesized cellulose–ZnO nanocomposites, the spectrum shows a combination of two sets of interesting diffraction peaks belonging to cellulose and ZnO which confirms the high crystallinity of the nanocomposite (Chen et al. 2008). The peaks marked * observed at $2\theta = 15.89$, 22.65 and 38.88° could be attributed to (110), (002) and (040) plane, respectively, of crystalline cellulose, whereas the other peaks at $2\theta = 32.01$, 34.60, 37.28, 47.62, 56.67, 63.47, and 68.11° are attributed to (100), (002), (101), (102), (110), (103), (112) and (201) crystal planes, respectively, indexed to the hexagonal wurtzite structure of ZnO (JCPDS file no. 36-1451). Comparing the spectrum of the nanocomposite and that of the isolated cellulose and ZnO NPs, it can be said that there were no peak shift or new peaks emanating from other sources except that of ZnO and cellulose matrix.

Morphological analysis

The morphological analyses of the corn cobs, isolated cellulose, ZnO NPs and the Cellulose–ZnO nanocomposites were carried out and shown in Fig. 3a–d. Figure 3a exhibits more disoriented fibril arrangement than Fig. 3b, an

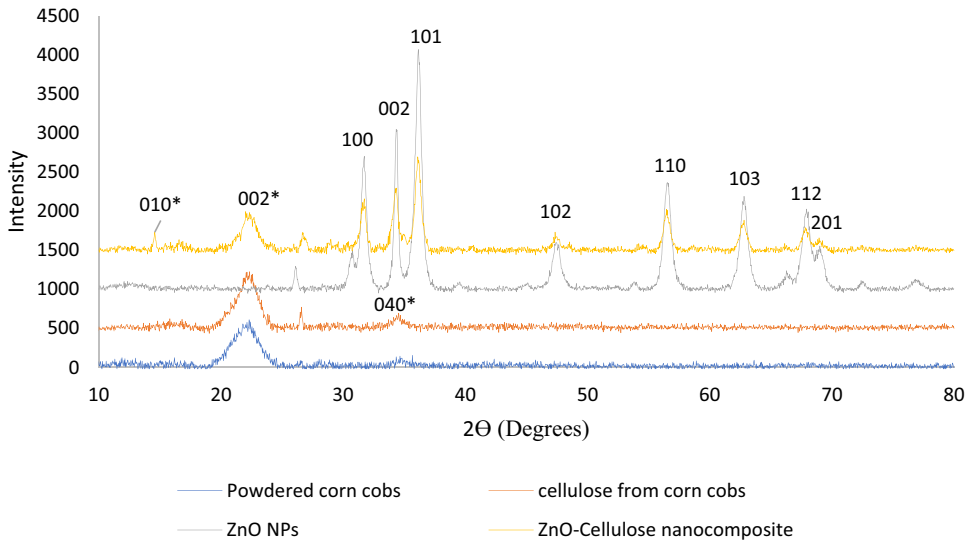

Fig. 2 XRD patterns of powdered corn cobs, cellulose, ZnO NPs and ZnO–cellulose nanocomposite

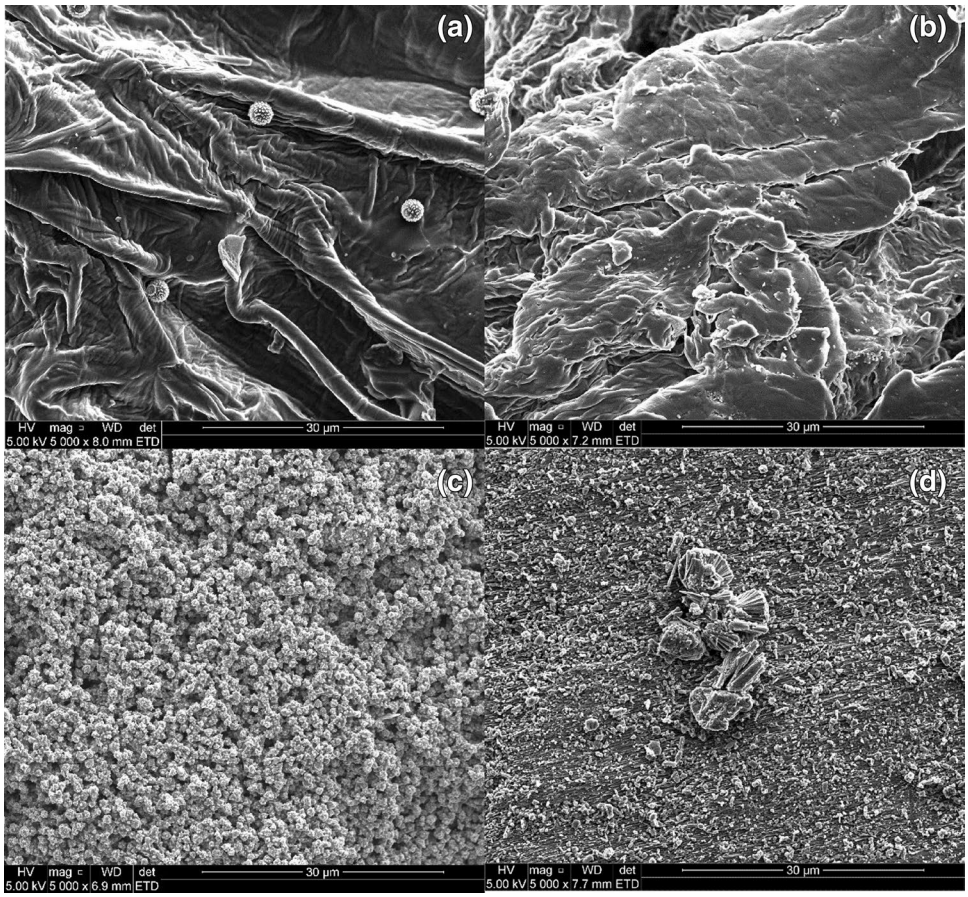

Fig. 3 SEM images of **a** corn cobs **b** cellulose from corn cobs **c** ZnO NPs **d** cellulose–ZnO nanocomposites

evidence that Fig. 3b is a more purified material which is the isolated cellulose. Corn cobs is a complex material that comprises fibres, carbohydrates, proteins, ash, lipids and moisture (Abubakar et al. 2016). The small spheres seen in Fig. 3a (corn cobs) may be as a result of orientation of some components of the corn cobs. Figure 3c reveals the ZnO seeds which is compact, whereas Fig. 3d shows the attachment of the ZnO seeds on the surface of the cellulose material in a low agglomerated manner. Such morphologies affect the properties of the nanocomposites and may lead to enhanced biological properties or rather become specific in some applications.

EDXS analysis of the materials

The EDXS analysis of the corn cobs, cellulose obtained from the corncobs, ZnO NPs synthesized using *Hibiscus* extract and the cellulose–ZnO nanocomposites are shown in Fig. 4a–d. In Fig. 4a, apart from the carbon and oxygen with weight percentages of 54% C and 45% O which represents the cellulose, there are other elements such as Cl, K and Na which are in minor quantities. The isolated cellulose as shown in Fig. 4b contains 53% C, 40% O, 2% Na, 5% Cl. The increased weight percentage of Cl and Na compared to the corn cobs may have been introduced by the bleaching agent. Figure 4c contains 56% Zn, 22% O and 21% C. It obviously shows ZnO NPs with higher percentage of Zn but the carbon content may have emanated from the plant extract. The cellulose–ZnO nanocomposite as depicted by the EDXS in Fig. 4d contains 13% Zn, 41% C, 39% O, 6% Na and 0.44% Cl. The elemental analyses and the Zn concentration showed that there was proper distribution of Zn on the surface of the cellulose. The EDX results support the SEM images shown in Fig. 3a–d where seeds of ZnO nanoparticles (Fig. 3c) were grown on the strands of the cellulose in an orderly manner (Fig. 3d).

TEM analysis

Different shapes of nanoparticles can be obtained depending on the mode of synthesis, the type of material used and the reaction conditions. The ZnO NPs prepared using the *Hibiscus* extract are rod like nanoparticles with width of about 90.83 nm and length 546.97 nm (Fig. 5a). The ZnO–cellulose nanocomposites on the other hand gave nanoparticles which were seen to be properly impregnated on the cellulose as spheroids with particle size of approximately 4.89 nm (Fig. 5b). The inset in Fig. 5b is the histogram

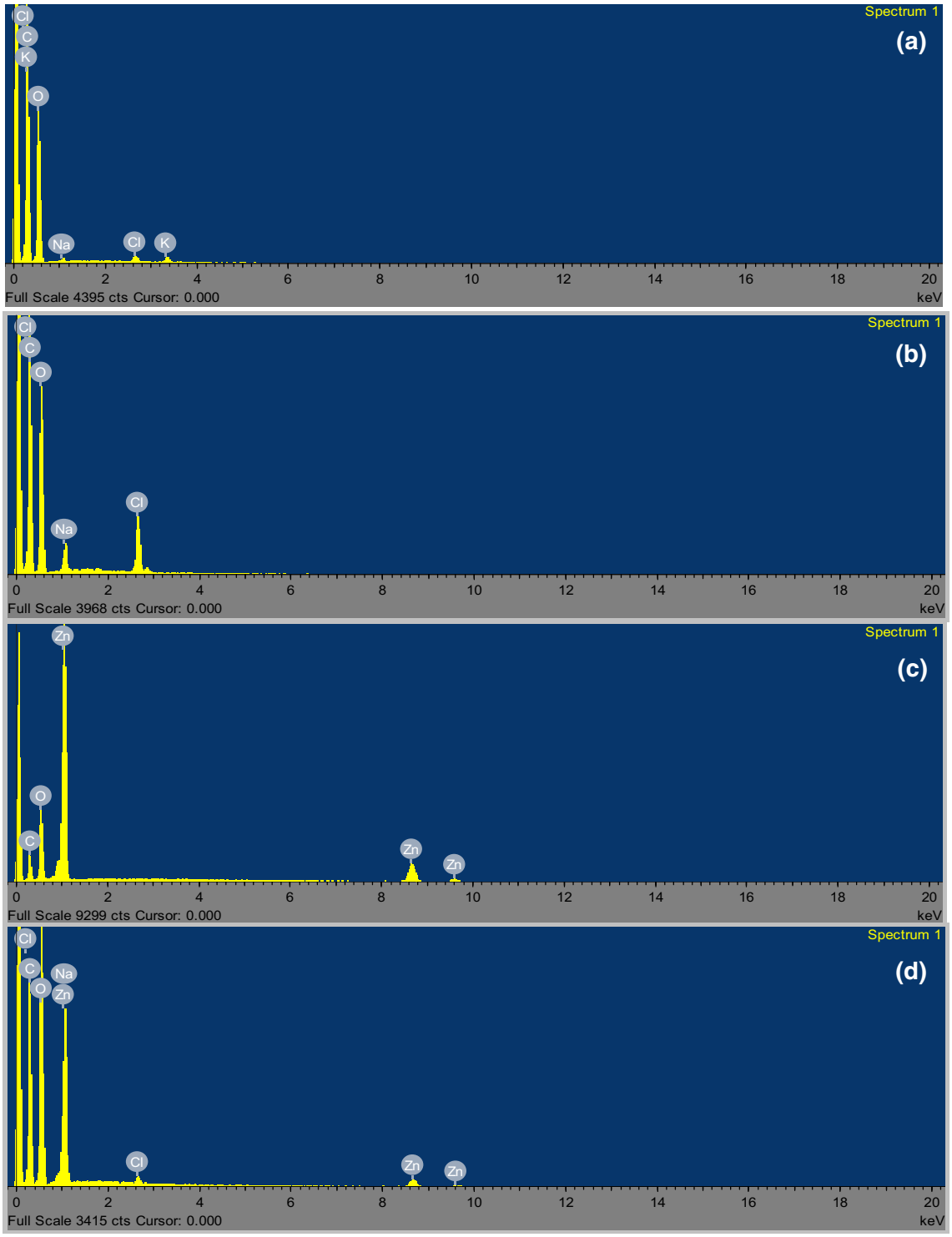

Fig. 4 EDXS spectra of **a** corn cobs **b** cellulose from corn cobs **c** ZnO NPs **d** cellulose–ZnO nanocomposite

which explains the average particle size (4.89 nm) obtained from image J software.

Typically, the concentration of Zn^{2+} in the nanocomposites greatly determines the morphologies and sizes of the nanomaterials as reported by Abdalkarim et al. (2018b). In their reports, the use of 2.5 mmol $ZnCl_2$ precursor compounds in the synthesis gave non-uniform rod-like and sheetlike morphologies of average size diameter 90 ± 13.5 nm, whereas higher concentration of Zn^{2+} in the

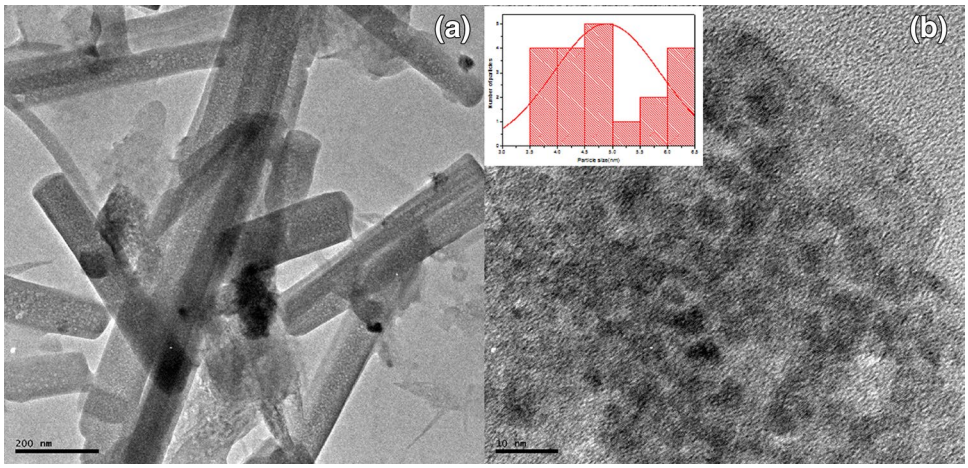

Fig. 5 TEM images of **a** ZnO NPs **b** cellulose–ZnO nanocomposites

Table 1 Zone of inhibition (mm) due to cellulose, ZnO NPs and ZnO/CNC against *Escherichia coli and Staphylococcus aureus*

Samples	*E. coli*	*S. aureus*
Cellulose from corn cobs	0	0
Hibiscus rosa-sinensis	14.50 ± 1.71	11.43 ± 2.85
ZnO-NPs	25 ± 0.40	15 ± 1.20
ZnO/CNC	35 ± 0.25	20 ± 0.45
Streptomycin (standard)	23 ± 1.05	23 ± 1.30

The values are mean and standard deviation of double replications

nanocomposites gave more sheetlike morphology with hexagonal-shaped ZnO nanosheets in the nanohybrids.

In this work, the use of the plant extract in the synthesis and the high concentration of the precursor compound obviously have led to the lower particle diameter and morphological change in the nanoparticles and nanocomposites compared to previous reports.

Antibacterial result

The antibacterial analyses of the cellulose, *Hibiscus rosa-sinensis* plant, synthesized ZnO NPs and the nanocomposite were carried out using *S. aureus* (Gram-positive) and *E. coli* (Gram-negative) as sample microorganisms by the Agar well diffusion method. From the results as shown in Table 1, the isolated cellulose on its own did not inhibit the growth of the bacteria. The plant material, ZnO NPs and the ZnO–cellulose nanocomposite showed good activity. However, the nanocomposite (ZnO/CNC) displayed improved antibacterial action more especially towards *E.coli*. This behavior could be attributed to the synergistic properties of the antibacterial effect of the plant material, crystallite size of ZnO and the contributing large surface area brought about by the cellulose and ZnONPs in the nanohybrid.

Abdalkarim et al. have also reported the inhibition of bacterial growth and reduction in bacterial amounts using cellulose nanocrystal–ZnO nanocomposites against *E.coli* and *S.aureus* (Abdalkarim et al. 2018a). Their results showed 3 and 4.5 mm zones of inhibition respectively for the bacteria though with diluted nanocomposites.

In another similar report also by Abdalkarim et al., zones of inhibition for antimicrobial effect of cellulose nanocrystals–ZnO nanohybrids against *E. coli* and *S. aureus* were also seen to be 3.0–5.1 mm and 4.1–4.9 mm, respectively (Abdalkarim et al. 2018b).

The simple antibacterial mechanism of action as reported by previous studies is that the nanoparticles target the surface of the microbes and disrupts their action (Azizi et al. 2013; Gunalan et al. 2012). Such process leads to the formation of reactive oxygen species (ROS) including super oxides (O^{2-}), hydrogen peroxide (H_2O_2) and hydroxyl radicals ($OH^{\cdot}$). The generation of ROS is a factor of the specific surface area of nanomaterials, hence larger surface area gives rise to more ROS and greater antibacterial activity (Padmavathy and Vijayaraghavan 2008). In the nanocomposites, there was dispersion of ZnO nanostructures due to the property effect of the cellulose polymer which gave rise to larger surface area and more generation of ROS. The generated ROS possibly cause the per-oxidation of the polyunsaturated phospholipids of the organism, penetration and direct damage to the cell wall (Wang et al. 2017; Sawai et al. 1996).

Moreover, further bactericidal mechanism could be due to electromagnetic interaction between the microorganism and the nanoparticles leading to interruption in the activities of the microorganisms (Yusof et al. 2019). The metal component oxidizes the microorganisms thereby deactivating their proteins, cell permeability and eventual death.

The higher activity shown towards *E. coli* than *S. aureus* may be due to the thick layer peptidoglycan cell wall of the *S aureus* (a Gram-positive bacteria) which is more difficult

towards penetration and destruction by the nanomaterials (Hu et al. 2020).

Conclusions

Cellulose was successfully isolated from corn cobs, zinc nanoparticles synthesized using leaf extract of *Hibiscus* plant and ZnO/CNC nanocomposite simultaneously made in all a simple and efficient biological route. The synthesized materials were characterized by different analytical techniques such as FTIR, XRD, SEM, EDX and TEM. XRD showed that ZnONPs has a hexagonal wurtzite structure, while the FTIR showed the different functional groups present in the nanomaterials. The morphological analysis gave an insight into the growth of zinc oxide seeds on the cellulose in a well-ordered manner. However, the incorporation of the zinc oxide nanoparticles into the cellulose affected the morphology from nanorods to conjugated spheres of approx. size of 4.89 nm. From the research work, the combination of ZnONPs with cellulose apparently improved the antibacterial functions especially towards the inhibition of *E. coli*. The standard drug, streptomycin gave an inhibition zone of 23 nm, whereas the ZnO/CNC gave an inhibition zone of 35 nm. This method involving cellulose and benign semi-conductor nanomaterials, therefore, is a good approach towards the development of cheaper yet more effective antibacterial agents due to interesting properties emanating from the combined materials.

Acknowledgements The authors acknowledge the management of Federal University of Petroleum resources Effurun for the platform that enabled this work.

Compliance with ethical standards

Conflict of interest The authors declare that there is no clash of interest associated with this work.

References

Abdalkarim SYH, Yu H-Y, Wang C, Yang L, Guan Y, Huang L, Yao J (2018a) Sheet-like cellulose nanocrystal-ZnO nanohybrids as multifunctional reinforcing agents in biopolyester composite nanofibers with ultrahigh UV-shielding and antibacterial performances. ACS Appl Bio Mater 1:727

Abdalkarim SYH, Yu H-Y, Wang C, Huang L-X, Yao J (2018b) Green synthesis of sheet-like cellulose nanocrystal–zinc oxide nanohybrids with multifunctional performance through one-step hydrothermal method. Cellulose 25(11):6446

Abderrahim B, Abderrahman E, Mohamed A, Fatima T, Abdesselam T, Krim O (2015) Kinetic thermal degradation of cellulose, polybutylene succinate and a green composite: comparative study. World J Environ Eng 3(4):110

Abubakar US, Yusuf KM, Safiyanu I, Abdullahi S, Saidu SR, Abdu GT, Indee AM (2016) Proximate and mineral composition of corn cob, banana and plantain peels. Int J food Sci Nutr 1:27

Adeyemi JO, Elemike EE, Onwudiwe DC (2019) ZnO nanoparticles mediated by aqueous extracts of Dovyalis caffra fruits and the photocatalytic evaluations. Mater Res Express 6:125091

Agrawal R, Espinosa HD (2011) Giant piezoelectric size effects in Zinc Oxide and Gallium Nitride nanowires. A first principles investigation. Nano Lett 11:790

Al-Snafi AE (2018) Chemical constituents, pharmacological effects and therapeutic importance of Hibiscus rosa-sinensis- A review. IOSR J Pharm 8:119

Awan F, Islam MS, Ma Y, Yang C, Shi Z, Berry RM, Tam KC (2018) Cellulose nanocrystal-ZnO nanohybrids for controlling photocatalytic activity and UV protection in cosmetic formulation. ACS Omega 3:12411

Azizi S, Ahmad MB, Hussein MZ, Ibrahim NA (2013) Synthesis, antibacterial and thermal studies of cellulose nanocrystal stabilized ZnO-Ag heterostructure nanoparticles. Molecules 18:6280

Börjesson M, Westman G (2015) Cellulose—fundamental aspects and current trends. Intech Books, London, pp 160–169

Chaudhuri SK, Malodia L (2017) Biosynthesis of zinc oxide nanoparticles using leaf extract of Calotropis gigantea: characterization and its evaluation on tree seedling growth in nursery stage. Appl Nanosci 7:512

Chen T, Zheng Y, Lin J-M, Chen G (2008) Study on the photocatalytic degradation of methyl orange in water using Ag/ZnO as catalyst by liquid chromatography electrospray ionization ion-trap mass spectrometry. J Am Soc Mass Spectrom 19:1003

Crabbe-Mann M, Tsaoulidis D, Parhizkar M (2018) Ethyl cellulose, cellulose acetate and carboxymethyl cellulose microstructures prepared using electrohydrodynamics and green solvents. Cellulose 25:1703

Du Y, Huang Z, Wu S, Xiong K, Zhang X, Zheng B, Nadimicherla R, Fu R, Wu D (2018) Preparation of versatile yolk-shell nanoparticles with a precious metal yolk and a microporous polymer shell for high-performance catalysts and antibacterial agents. Polymer 137:200

Elemike EE, Fayemi OE, Ekennia AC, Onwudiwe DC, Ebenso EE (2017) Silver nanoparticles mediated by costus afer leaf extract: synthesis, antibacterial, antioxidant and electrochemical properties. Molecules 22:701

Elemike EE, Onwudiwe DC, Wei L, Chaogang L, Zhiwei Z (2019) Synthesis of nanostructured ZnO, AgZnO and the composites with reduced graphene oxide (rGO-AgZnO) using leaf extract of Stigmaphyllon ovatum. J Environ Chem Eng 7:103190

Food Standards Agency. Current EU approved additives and their E Numbers 2014. www.food.gov.uk/science/additives/enumberlist

Fu F, Li L, Liu L, Cai J, Zhang Y, Zhou J, Zhang L (2015) Construction of cellulose based ZnO nanocomposite films with antibacterial properties through one-step coagulation. ACS Appl Mater Interfaces 7:2606

Gunalan S, Rajeswari S, Venckatesh R (2012) Green synthesized ZnO nanoparticles against bacterial and fungal pathogens. Prog Nat sci Mater Int 22(6):700

Hu X, Xu X, Fu F, Yang B, Zhang J, Zhang Y, Touhid SSB, Liu L, Dong Y, Liu X, Yao J (2020) Synthesis of bimetallic silver-gold nanoparticle composites using a cellulose dope: tunable nanostructure and its biological activity. Carbohydr Polym 248:116777

Jawada AH, Mohammed SA, Mastuli MS, Abdullah MF (2018) Carbonization of corn (Zea mays) cob agricultural residue by onestep activation with sulfuric acid for methylene blue adsorption. Desalin Water Treat 118:351

Kalia S, Kaith BS, Kaur I (2009) Pretreatments of natural fibers and their application as reinforcing material in polymer composites—A review. Polym Eng Sci 49(7):1272

Kim J, Yun S, Ounaies Z (2006) Discovery of cellulose as a smart material. Macromolecules 39:4206

Lefatshe K, Muiva CM, Kebaabetswe LP (2017) Extraction of nanocellulose and in-situ casting of ZnO/cellulose nanocomposite with enhanced photocatalytic and antibacterial activity. Carbohyd Polym 164:308

Lennholm H, Henriksson G (2007) In: Ek M, Gellerstedt G, Henriksson G (eds) Fiber and polymer technology, Ljungberg Textbook Stockholm, KTH, pp 72–102

Li R, Zhang L, Xu M (2012) Novel regenerated cellulose films prepared by coagulating with water: structure and properties. Carbohydr Polym 87:100

Martins NCT, Freire CSR, Neto CP, Silvestre AJD, Causio J, Baldi G, Sadocco P, Trindade T (2013) Antibacterial paper based on composite coatings of nanofibrillated cellulose and ZnO. Colloids Surf A 417:119

Matharu RK, Ciric L, Edirisinghe M (2018) Nanocomposites: suitable alternatives as antimicrobial agents. Nanotechnol 29:282001

Morawski AW, Kusiak-Nejman E, Przepiórski J, Kordala R, Pernak J (2013) Cellulose-TiO_2 nanocomposite with enhanced UV–Vis light absorption. Cellulose 20:1300

Mun S, Ko H-U, Zhai L, Min S-K, Kim H-C, Kim J (2016) Enhanced electromechanical behavior of cellulose film by zinc oxide nanocoating and its vibration energy harvesting. Acta Mater 114:6

Naseer M, Aslam U, Khalid B, Chen B (2020) Green route to synthesize Zinc Oxide Nanoparticles using leaf extracts of Cassia fistula and Melia azadarach and their antibacterial potential. Sci Rep 10:9055

Padmavathy N, Vijayaraghavan R (2008) Enhanced bioactivity of ZnO nanoparticles—an antimicrobial study. Sci Technol Adv Mat 9(3):35010

Rayung M, Ibrahim NA, Zainuddin N, Saad WZ, Razak NIA, Chieng BW (2014) The effect of fiber bleaching treatment on the properties of poly(lactic acid)/oil palm empty fruit bunch fiber composites. Int J Mol Sci 15:14742

Ruban P, Gajalakshmi K (2012) In vitro antibacterial activity of Hibiscus rosa-sinensis flower extract against human pathogens. Asian Pac J Trop Biomed 2(5):403

Sawai J, Kawada E, Kanou F, Igarashi H, Hashimoto A, Kokugan T, Shimizu M (1996) Detection of active Oxygen generated from ceramic powders having antibacterial activity. J Chem EngJpn 29(4):633

Sharma ND, Landis CM, Sharma P (2010) Piezoelectric thin-film superlattices without using piezoelectric materials. J Appl Phys 108:024304

Siddiqi KS, Rahman AU, Tajuddin AH (2018) Properties of Zinc Oxide nanoparticles and their activity against microbes. Nanoscale Res Lett 13:141

Sirelkhatim A, Mahmud S, Seeni A, Kaus NHM, Ann LC, Bakhori SKM, Hasan H, Mohamad D (2015) Review on Zinc Oxide nanoparticles: antibacterial activity and toxicity mechanism. Nano-Micro Lett 7(3):242

Sirviö JA, Visanko M, Hildebrandt NC (2017) Rapid preparation of all-cellulose composites by solvent welding based on the use of aqueous solvent. Eur Polymer J 97:298

Trilokesh C, Uppulur KB (2019) Isolation and characterization of cellulose nanocrystals from jackfruit peel. Sci Rep 9:16709

Ul-Islam M, Khattak WA, Ullah MW, Khan S, Park JK (2014) Synthesis of regenerated bacterial cellulose-zinc oxide nanocomposite films for biomedical applications. Cellulose 21:447

Vartiainen J, Pöhler T, Sirola K, Pylkkänen L, Alenius H, Hokkinen J (2011) Health and environmental safety aspects of friction grinding and spray drying of microfibrillated cellulose. Cellulose 18:786

Wang C, Shaw LL (2014) On synthesis of Fe_2SiO_4/SiO_2 and Fe_2O_3/SiO_2 composites through sol–gel and solid-state reactions. J Sol-Gel Sci Technol 72:614

Wang TY, Libardo MDJ, Angelesoza AM, Pellois JP (2017) Membrane oxidation in cell delivery and cell killing applications. ACS Chem Biol 12(5):1182

Wang D-C, Yang X, Yu H-Y, Gu J, Qi D, Yao J, Ni Q (2020) Smart nonwoven fabric with reversibly dual-stimuli responsive wettability for intelligent oilwater separation and pollutants removal. J Haz Mater 383:121123

Yusof HM, Mohamad R, Zaidan UH, Rahman NAA (2019) Microbial synthesis of zinc oxide nanoparticles and their potential application as an antimicrobial agent and a feed supplement in animal industry: a review. J Anim Sci Biotechnol 10:57

Zheng J, Choo K, Bradt C, Lehou R, Rehmann L (2014) Enzymatic hydrolysis of steam exploded corncob residues after pretreatment in a twin-screw extruder. Biotechnol Rep 3:107

Zou W, Chen Y, Zhang X, Li J, Sun L, Gui Z, Du B, Chen S (2018) Cytocompatible chitosan based multi-network hydrogels with antimicrobial, cell antiadhesive and mechanical properties. Carbohydr Polym 202:257